BULLETIN OF BIOMATHEMATICS

Bulletin of Biomathematics, 2023, 1(1), 40–57

https://bulletinbiomath.org
ISSN Online: 2980-1869 / Open Access
https://doi.org/10.59292/bulletinbiomath.2023003

RESEARCH PAPER

Numerical investigations and simulation of calcium distribution in the alpha-cell

Tejaswi Singh [1,‡], **Vaishali** [1,*,‡] **and Neeru Adlakha** [1,‡]

[1]Sardar Vallabhbhai National Institute of Technology, Surat, Gujarat 395007, India

*Corresponding Author
‡iittejaswi@gmail.com (Tejaswi Singh); d20ma002@amhd.svnit.ac.in (Vaishali); nad@amhd.svnit.ac.in (Neeru Adlakha)

Abstract

The α-cells are a part of islets of Langerhans located in the pancreas and are responsible for glucagon secretion. Calcium signaling is crucial for the regulation of the functions and structure of these α-cells and the same is still not well understood. Here a mathematical model is framed to obtain more insights into calcium signaling in α-cells. The non-linear reaction-diffusion equation for calcium signaling along with boundary conditions is employed to propose the model for a one-dimensional steady-state case. The numerical solutions were obtained using the Newton-Raphson method and the cubic spline method. The combination of Newton-Raphson and cubic spline has proved to be quite effective in numerical simulations and in generating deeper insights into calcium regulation in an α-cell under various conditions. The results provide information about changes in source influx, buffers, ER leak, and SERCA pump leading to disturbances in calcium homeostasis, which can be responsible for the development of diabetes and other metabolic disorders.

Keywords: Cubic spline method; Newton-Raphson method; calcium distribution; ER leak; SERCA

AMS 2020 Classification: 92B05; 92C37; 65D07; 34A45

1 Introduction

In order to maintain normal physiology and metabolism, calcium homeostasis mechanisms regulate ionized plasma calcium (Ca^{2+}) concentration in the human body within a specific range. The cytosolic calcium is kept at a very low-level [1]. The cytosolic calcium level can rise by releasing calcium from intracellular reserves and bringing calcium in from external sources. The calcium level within the α-cell regulates biophysical processes like the formation and secretion of glucagon hormone [2]. The free calcium level inside the α-cell is maintained at 0.1 μM under resting conditions. The α-cells have pyramidal shape and size about 8 μm in diameter and they appear in groups [3]. Due to the electrically excitable nature, the α-cells continuously generate overshooting action potentials when the release of glucagon is induced at a low concentration of glucose.

➤ **Received:** 27.03.2023 ➤ **Revised:** 22.04.2023 ➤ **Accepted:** 24.04.2023 ➤ **Published:** 30.04.2023

Voltage-gated Na^+ and Ca^{2+} channels are crucial for the upstroke of action potentials. Voltage-gated Ca^{2+} channels (VGCCs) are opened by the discharge of high-voltage action potentials allowing extracellular calcium to enter the cytosol. As a result, the number of intracellular calcium rises, which triggers the glucagon granule exocytosis process thereby leading to the fusion of hormone-containing granules with cell membranes and the secretion of the hormones contained inside. Glucagon secretion is inhibited as blood glucose levels rise. This is most likely accomplished via a decrease in the activity of P/Q-type calcium channel of α-cells and by SERCA pump, which stimulates Ca^{2+}-sequestration into the ER [4]. In stable conditions, the glucose level lies between 70 to 180 mg/dl, i.e., normoglycemia. If it falls below 70 mg/dl, the body experiences hypoglycemia. The pancreatic α-cells then secrete glucagon, which causes the liver to release glucose back into the bloodstream, stabilizing its concentration. Contrarily, hyperglycemia occurs when blood sugar levels rise above 180 mg/dl. The pancreatic β-cells then secrete insulin, which causes fatty tissue to absorb glucose to bring the blood sugar level back to normal [5]. A lot of similar secretory machinery has been found in β and α-cells [6]. Disruptions in these mechanisms are the key factor in the growth of diabetes, which is commonly divided into two categories: Type-1 diabetes and Type-2 diabetes [5].

Many researchers and scientists have developed a variety of mathematical models for studying calcium signaling in different cells like myocytes [7–11], neurons [12–26], astrocytes [27–31], hepatocytes [32–34], fibroblasts [35–38], lymphocytes [39, 40], oocytes [41–48], acinar cells [49–51], dendritic spines [52], etc. In order to understand the kinetics of calcium signaling in endothelial cells, Wiesner et al. [53] constructed a model which gives a mathematical explanation of how calcium affects the ability of the endothelial cell to transmit signals. A mathematical model was created by Handy [27] to investigate the effects of calcium pumps, channels, ER leak, SERCA, and other elements on calcium dynamics in astrocytes. They proposed that modifications to this parameter's ratio had a direct impact on the cytosolic calcium levels in astrocyte cells. The calcium dynamics in a neuron have been examined by Futagi and Kitano [54]. They computationally analyzed the effect of the ryanodine receptor and how it can cause the fluctuation in the calcium profile. Proposing a finite element model, Tewari and Pardasani [19–23] demonstrated calcium distribution in neurons. They considered a number of buffers, including EGTA, BAPTA, Troponin, and Calmodulin for their study. A mathematical model has been created by Jha et al. [28–31] to investigate the calcium advection and diffusion phenomenon in astrocytes. This model includes an advection-diffusion equation, suitable boundary conditions, and physiological factors like diffusion coefficient, buffers and VGCC. To acquire the numerical results, they used the finite element method. Naik and Pardasani [41–46] used the same technique to investigate the calcium distribution in oocyte cells while buffer, VGCC, and receptor were present. Due to these variables, they saw a considerable variation in calcium profiles. Pathak and Adlakha [7–9] investigated the finite element model in order to confirm the physiological mechanism of calcium homeostasis in myocytes by considering factors such as a leak, pump and excess buffer. They discovered that while leaks help to increase calcium concentration, buffers are important to lower it. In recent years, some advancements have also been made by researchers in the field of computational modeling. Joshi and Jha [55, 56] considered the fractional reaction-diffusion equation to study the physiological phenomenon in depth in neurons. Additionally, they expanded their model to a two-dimensional study and correlated the findings with the physiology of neurodegenerative disorders [57, 58].

Nowadays, it is commonly acknowledged that insufficient pancreatic hormone secretion is the major cause of the emergence of diabetes [59]. Impaired insulin profile has been the main topic of study these days. Several computational and theoretical studies have been devoted to the

exocytosis and electrical behavior of β-cell [60, 61], but there is relatively little information available regarding the modeling of the calcium signaling in pancreatic α-cell. Diderichsen and Gopel [62] established a mathematical model of electrical activity based on the ion channel properties of α-cells found on the surface of healthy mouse islets in 2006. Additionally, their model was revised by Watts and Sherman [6] in 2014 to include calcium dynamics and secretion. Similar findings of secretion, calcium dynamics and electrical activity were described theoretically by Fridlyand and Philipson [63] in 2012. Exocytosis and secretion were mostly analyzed [6, 62, 63] as an impact of electrical activity, although the primary goal was on the modulation of α-cell electrical activity. A mathematical model was constructed by Montefusco and Pedersen [64] to test the α-cells electrical activity modulations that result in glucose administration. They describe the intracellular calcium profile with a focus on simulating calcium concentrations in the microdomains implicated in the release of glucagon. Briant et al. [4] investigated the mechanisms behind metabolic regulation of glucagon secretion of α-cells with the help of a mathematical model. They also examined the paracrine and intrinsic mechanisms of α-cells. Brereton et al. [65] in their work concluded that inter-islet communication is restored by both islet architecture and cellular functions. It is also responsible for glucose homeostasis in diabetes. González-Vélez et al. [2] investigated the importance of calcium and glucose maintaining the secretion of glucagon hormone through α-cells. They also established that the secretion of glucagon is potentiated by calcium variation in comparison to a constant level of intracellular calcium. The model emphasized the exocytosis of α-cell and gave the tools helping in the study of modulators involved in glucagon secretion. Moede et al. [66], in their research work, gave the relationship of α and β-cells. Their main focus was the hormones secreted by α-cells, such as acetylcholine and glucagon. The inter-relationship of α and β-cells is affected by different architectures of the islet in various species.

From the literature survey, it can be observed that glucagon secretion is responsible for maintaining the glucose level and it depends on the calcium signaling of the cells. Most of the studies found in the literature are based on either the electrical activity of the α-cells [6, 62, 63] or they describe the metabolic regulation of glucagon secretion theoretically [2, 4]. On the other hand, several attempts have been made to solve the linear form of the reaction-diffusion model for the other cells using different mathematical techniques like FEM and FVM [23, 31, 32, 46]. It has been noted that no attempts have been made to analyze the non-linear calcium distribution involving SERCA pump and ER leak in an α-cell. Furthermore, little is known about how numerous factors including diffusion, influx, the SERCA pump and ER leak affect calcium signaling in α-cells. The previous studies on calcium signaling in various cells with the help of the finite element method used linear interpolation functions which required a large number of elements to achieve the desired accuracy. In the present paper, the above-mentioned issues are addressed by developing a mathematical model of calcium signaling in an α-cell. The non-linear reaction-diffusion equation along with boundary conditions is employed to construct a model in the form of a boundary value problem. The numerical results are calculated by using the combination of the cubic spline method and the Newton-Raphson method. The cubic spline method is employed to obtain an approximation of the field variable in the cell domain. The Newton-Raphson approach has been implemented to effectively obtain the numerical solution of the non-linear equations. The way the study is performed is as follows: the steady state distribution of calcium in an α-cell is modeled by a non-linear reaction-diffusion equation in Section 2. In Section 3, the calcium profile for various physiological parameters is discussed. Section 4 completes our discussion with conclusions. Finally, in Section 5, the algorithms of the cubic spline method and Newton-Raphson method are given.

2 Construction of the mathematical model

The proposed model incorporates two mechanisms of calcium influx due to an ER leak and outflow caused by the SERCA pump. We begin by assuming a single well-mixed pool (like the cytoplasm of the α-cell) where a bimolecular association interaction of calcium and buffer takes place. The calcium-buffer binding and unbinding equation is given by [67, 68]:

$$Ca^{2+} + B \underset{k^-}{\overset{k^+}{\rightleftharpoons}} CaB, \tag{1}$$

where Ca^{2+}, B and CaB denote the free calcium, free buffer and calcium-bound buffer respectively. The terms k^+ and k^- are the rate constants for association and dissociation, respectively.
The required equation for analyzing the calcium regulation in an α-cell is given as follows [61, 64, 67, 68]:

$$\frac{\partial [Ca^{2+}]}{\partial t} = D_{Ca}\nabla^2[Ca^{2+}] - k_i^+[B_i]_\infty([Ca^{2+}] - [Ca^{2+}]_\infty) + J_{leak} - J_{SERCA}, \tag{2}$$

where D_{Ca} is the diffusion coefficients of free Ca^{2+} and J_{leak} and J_{SERCA} represent the ER leak and SERCA pump flux, respectively and given as follow:

$$J_{leak} = P_{ER}([Ca^{2+}]_{ER} - [Ca^{2+}]), \tag{3}$$

where P_{ER} leak permeability out of the ER and $[Ca^{2+}]_{ER}$ is the free calcium concentration in ER.

$$J_{SERCA} = P_{SERCA}^{max}\frac{[Ca^{2+}]^2}{k_{pump}^2 + [Ca^{2+}]^2}, \tag{4}$$

where P_{SERCA}^{max} and k_{pump} are the maximum pumping rate and half maximum pump activity of SERCA pump, respectively [64, 69].

For one-dimensional steady-state case in cartesian coordinates, the equation (2) is given by:

$$\frac{\partial^2[Ca^{2+}]}{\partial x^2} - \frac{k^+[B]_\infty}{D_{Ca}}([Ca^{2+}] - [Ca^{2+}]_\infty) + \frac{P_{ER}}{D_{Ca}}([Ca^{2+}]_{ER} - [Ca^{2+}]) - \frac{P_{SERCA}^{max}}{D_{Ca}}\frac{[Ca^{2+}]^2}{k_{pump}^2 + [Ca^{2+}]^2} = 0. \tag{5}$$

The source term of the calcium is assumed at the point x=0 μm, thus the flux boundary is given as follows [68]:

$$\lim_{x\to 0}\left(-D_{Ca}\frac{\partial [Ca^{2+}]}{\partial x}\right) = \sigma_{Ca}. \tag{6}$$

The other end boundary is assumed at the resting state i.e., the background calcium concentration is assumed at that point and expressed as follows:

$$\lim_{x\to\infty}[Ca^{2+}] = 0.1\mu M. \tag{7}$$

Re-writing equation (5), we get:

$$\frac{\partial^2 y}{\partial x^2} - Ay - B\frac{y^2}{k_{pump}^2 + y^2} + C = 0, \tag{8}$$

where

$$A = \frac{k^+[B]_\infty + P_{ER}}{D_{Ca}},$$

$$B = \frac{P_{SERCA}^{max}}{D_{Ca}},$$

$$C = \frac{k^+[B]_\infty[Ca^{2+}]_\infty + P_{ER}[Ca^{2+}]_{ER}}{D_{Ca}},$$

and y denotes the $[Ca^{2+}]$. In past studies, various research workers have used the finite element method with linear interpolation functions. The linear interpolation functions give linear approximation within each subdomain/interval giving a polygonal curve for the field variable as an approximation to a real/smooth curve within the whole domain/cell. Therefore to achieve good approximation the smaller step size is taken to discretize the domain in a larger number of elements/intervals to make a polygonal curve very close to the smooth curve of the field variable in the domain/cell to achieve good accuracy. Here the cell size is very small i.e. few microns. Further, the cubic splines are superior to linear interpolation as it satisfies higher-order continuity conditions to give smooth curves and its order of approximation is higher than the order of approximation of linear interpolation functions. Thus, we have two options to achieve good approximation: (i) Use linear interpolation functions and take a smaller step size to divide the domain into a larger number of intervals/elements or (ii) Use higher order interpolation functions like cubic splines and divide the domain in a smaller number of intervals/elements. The first option requires a larger number of elements which in the case of the nonlinear system becomes very complicated and requires large computational efforts. The second option of using cubic splines requires a smaller number of elements leading to a smaller number of nonlinear equations thereby reducing complications and requiring less computational effort but more mathematical manipulations. Here we use the second option and discretize the cell into eight equal elements to obtain better results by solving a more realistic model. The cubic spline method [70, 71] has been applied to solve the model given by equation (8) and the boundary conditions equation (6) and (7). Thus, equations for the internal nodes are given as follows:

$$\frac{h}{6}N_{j-1} + \frac{2h}{3}N_j + \frac{h}{6}N_{j+1} = \frac{y_{j+1} - 2y_j + y_{j-1}}{h}, \tag{9}$$

where

$$N_j = Ay_j + B\frac{y_j^2}{k_{pump}^2 + y_j^2} - C, \tag{10}$$

where $j = 1, 2, 3, \cdots, 7$ and $h = x_j - x_{j-1}$.
Substituting the value of equation (10) in equation (9) and after rearranging, we get:

$$\left(\frac{Ah}{6} - \frac{1}{h}\right) y_{j-1} + 2\left(\frac{Ah}{3} + \frac{1}{h}\right) y_j + \left(\frac{Ah}{6} - \frac{1}{h}\right) y_{j+1} + \frac{Bh}{6}\left(\frac{y_{j-1}^2}{k_{pump}^2 + y_{j-1}^2} + 4\frac{y_j^2}{k_{pump}^2 + y_j^2} + \frac{y_{j+1}^2}{k_{pump}^2 + y_{j+1}^2}\right) - Ch = 0, \tag{11}$$

where $j = 1, 2, 3, \cdots, 7$.
Condition for the right boundary is obtained by using equation (7):

$$y_8 - 0.1 = 0. \tag{12}$$

Applying the cubic spline method on equation (6), the condition for the left boundary is given as follows:

$$-\frac{h}{3}N_j - \frac{h}{6}N_{j+1} + \frac{y_{j+1} - y_j}{h} = -\frac{\sigma_{Ca}}{D_{Ca}}, \tag{13}$$

$$N_0 = \frac{3}{h^2}(y_1 - y_0) - \frac{1}{2}N_1 + \frac{3}{h}\frac{\sigma_{Ca}}{D_{Ca}}. \tag{14}$$

Combining equations (11), (12) and (14), a non-linear system of 9 equations has been obtained. A MATLAB program of the Newton-Raphson method for the nonlinear system has been developed to solve the obtained system. In Table 1, biophysical parameters and corresponding numerical data are presented.

Table 1. Biophysical parameters and numerical data [64, 68, 69]

Notation	Name of the parameter	Numerical value
D_{Ca}	Diffusion Coefficient	250 $\mu m^2/sec$
K^+	Association rate of EGTA	1.5 $\mu M/sec$
B_∞	EGTA	5 μM
P_{ER}	Calcium leak permeability of ER	0.0001 $/sec$
P_{SERCA}^{max}	Maximum pumping rate of SERCA	0.105 $\mu M/sec$
k_{pump}	Half-maximum pumping rate of SERCA	0.5 μM
$[Ca^{2+}]_\infty$	Cytosolic calcium at rest	0.1 μM
$[Ca^{2+}]_{ER}$	Calcium concentration in ER	22.8 μM
σ_{Ca}	Source influx	15 pA

3 Results and discussion

The data of the parameters listed in Table 1 were used to compute numerical solutions. The profiles for calcium concentration with respect to space for different conditions have been plotted. Figure 1 depicts the cytosolic calcium of the α-cell with respect to space. It can be observed from the figure that concentration is initially high near the source influx and then gradually drops as we move away from the source. However, at the other end, it attains its equilibrium value which is 0.1 μM. Active pumps and buffers within the α-cell were the cause of the change in calcium concentration with regard to space.

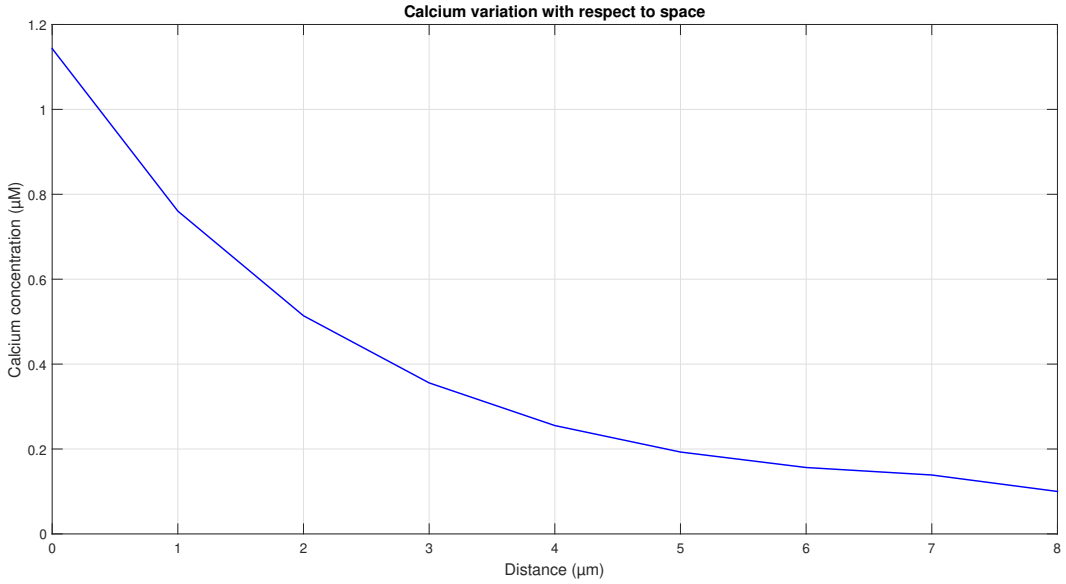

Figure 1. Calcium concentration for standard values of parameters given in Table 1

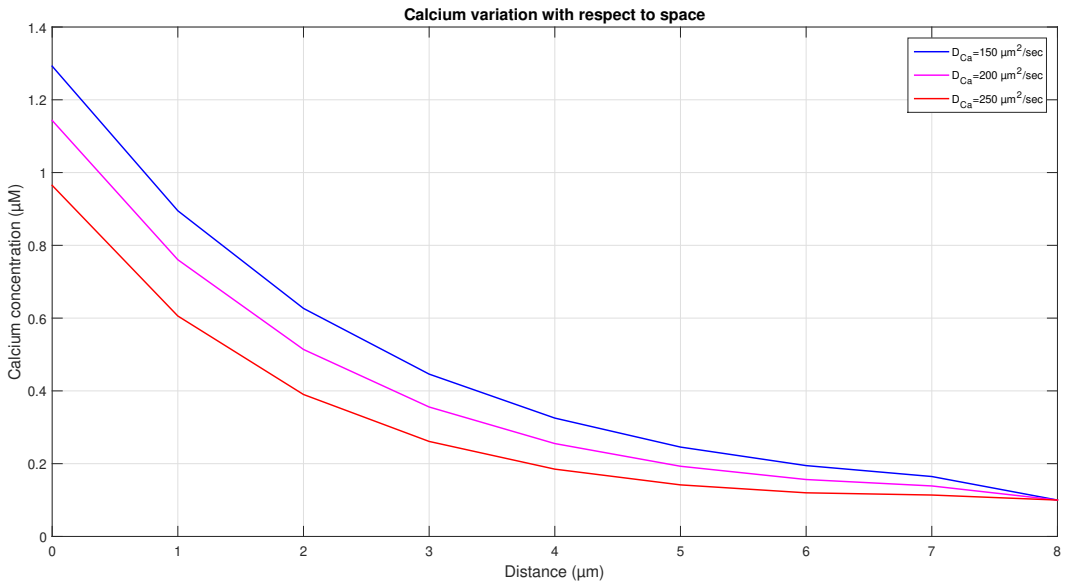

Figure 2. Calcium concentration for different values of diffusion coefficients

The spatial variation in calcium concentration as the diffusion coefficient values change from 150 to 200 and 200 to 250 $\mu m^2/sec$ is shown in Figure 2. The diffusion coefficient is defined as the amount of diffusing substance moved per unit area per unit of time from one portion of the cell to another. This indicates that calcium ions will flow quickly from the apical to the basal portion of the cell for a larger value of D_{Ca}. For D_{Ca} = 250 $\mu m^2/sec$, less free calcium accumulates in the space as more calcium is carried through the cell. Therefore, the concentration of calcium decreases as the magnitude of the diffusion coefficient increases. The amount of free calcium is clearly inversely proportional to the diffusion coefficient, as seen in the graph.

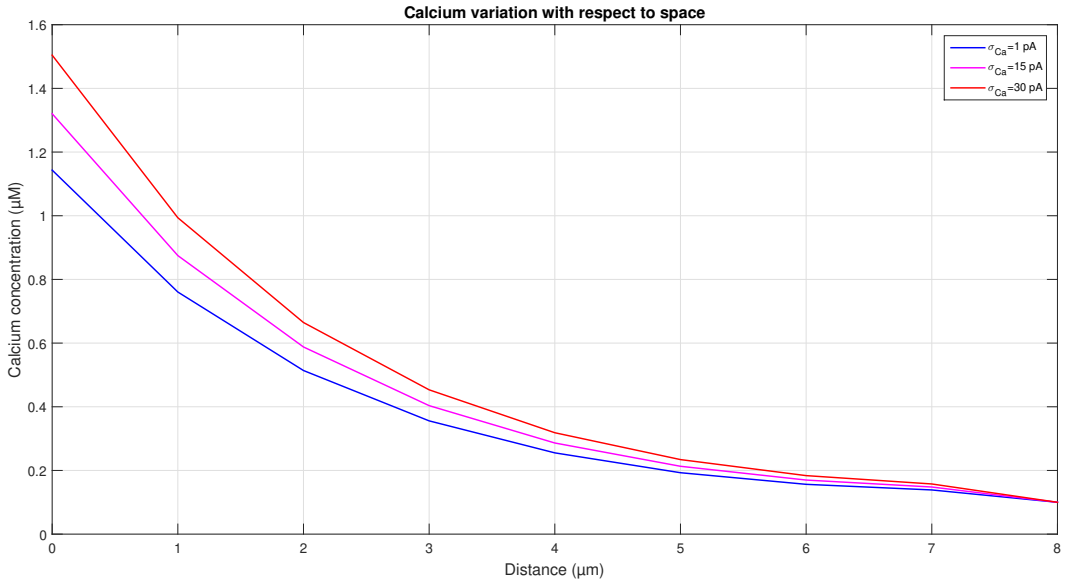

Figure 3. Calcium concentration for different values of source influx

The spatial change in calcium concentration when the value of source amplitude σ_{Ca} is 1, 15 and 30 pA respectively is shown in Figure 3. The unit of characteristic amplitude current passing through a channel is pico amperes (pA). The open channel permits ions to pass and is measured as current. As the source amplitude's value increases, more calcium is released into the cytosol. Thus it leads to an increase in the concentration of free calcium. It can be seen from Figure 3 that the concentration of calcium is 1.1, 1.3 and 1.5 μM respectively for 1, 15 and 30 pA source amplitude at the mouth of a point source and thereafter it decreases uniformly up to 0.1 μM. The appropriate experimental results are still not available for comparison, but however, the outcomes of the suggested model are consistent with biological facts.

Figure 4 represents the spatial change in calcium profile for various EGTA buffer quantities. It can be noticed that different quantities of buffers have different effects on the calcium profile. The maximum calcium concentration occurs for EGTA = 10 μM and the minimum calcium concentration occurs for EGTA = 50 μM. In all three EGTA buffers above with different quantities, the concentration of calcium decreases with an increase in the concentration of cytosolic buffer inside the α-cell.

Figure 5 demonstrates the effect of different pumping rates on the calcium concentration inside the α-cell. The graph shows three different pumping rates. When the pumping rate P^{max}_{SERCA} is 0.1 $\mu M/sec$, the cytosolic calcium is higher and the concentration begins to decline as the pumping rate increases. Calcium concentration also decreases with an increase in the distance of the cell from the source.

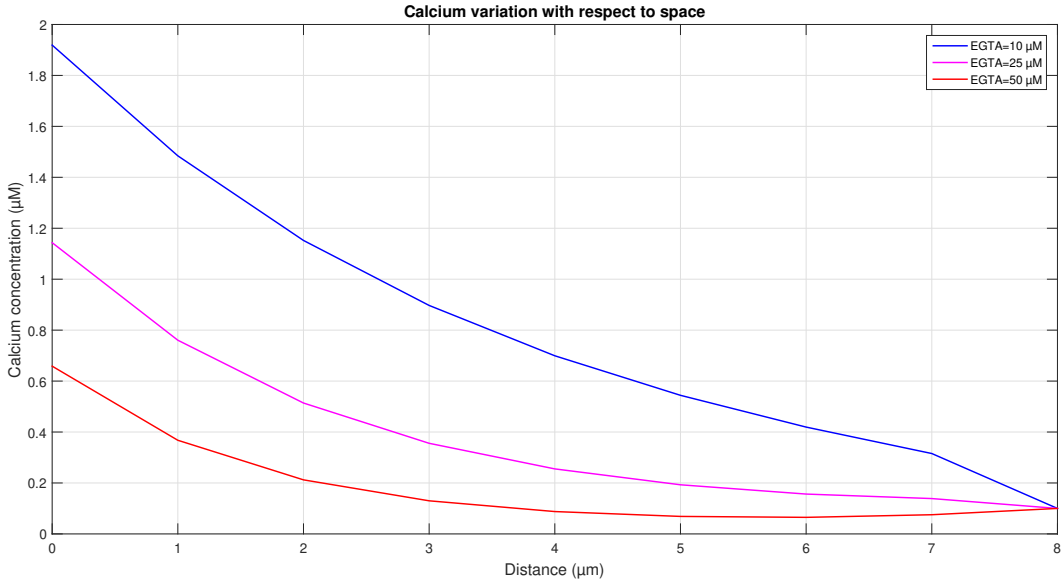

Figure 4. Calcium concentration for different values of buffer concentration(EGTA buffer)

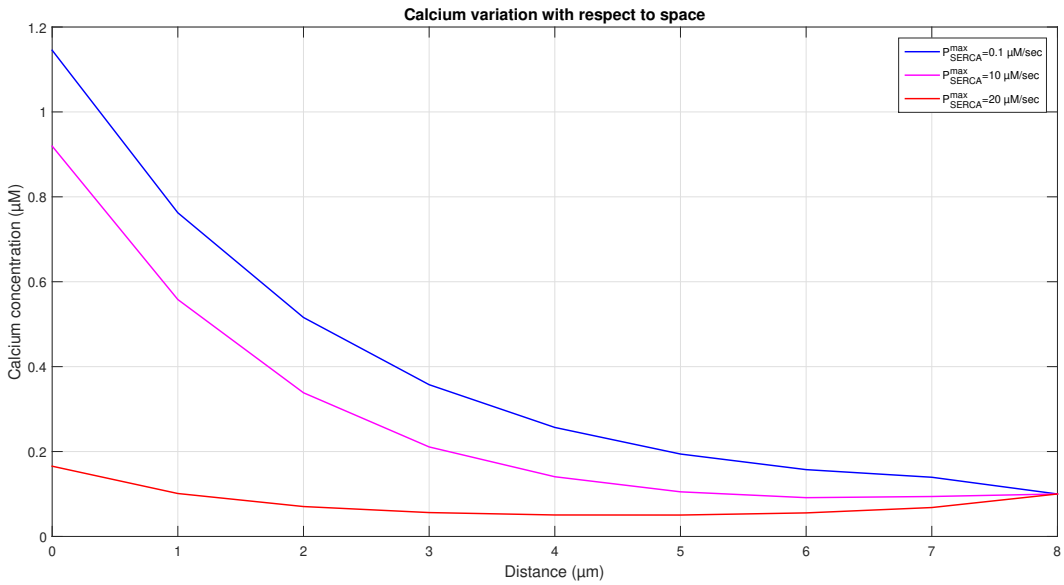

Figure 5. Calcium concentration for different pumping rates of SERCA

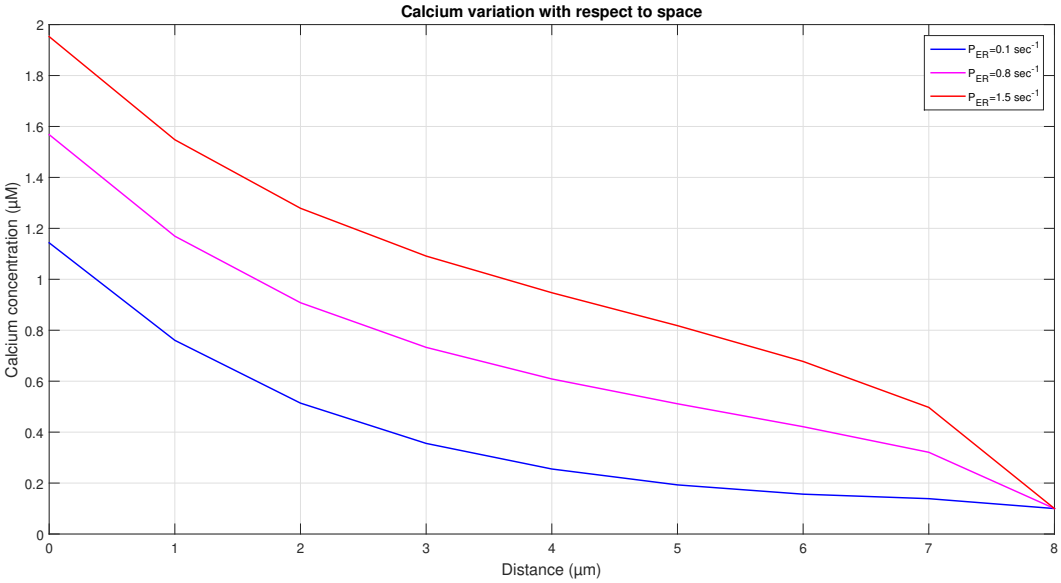

Figure 6. Calcium concentration for different values of ER leak

Figure 6 demonstrates the effect of different leak rates (P_{ER}). Here with an increase in the distance from the source of the cell, the calcium concentration inside the cell decreases. The gaps observed among the curves in the figure indicate that leak helps in raising the cytosolic calcium with the increase in leak rate. The figure also shows how altering the leak rates causes variations in calcium concentration.

4 Conclusion

A one-dimensional steady-state model for calcium distribution has been proposed and effectively used to examine the roles of different factors like EGTA buffers, source influx, leak, pump, etc. on the cytosolic calcium concentration of the α-cell. The combination of the cubic spline and Newton-Raphson method has proved to be effective for solving non-linear reaction-diffusion and performing numerical simulations to obtain valuable results. The following conclusions have been drawn:

i. The buffers and pumps are crucial in lowering calcium levels in an α-cell.
ii. The source influx and leak are crucial in raising the calcium concentration in an α-cell.
iii. The cell has a beautiful mechanism for balancing this calcium concentration by elevating and reducing mechanisms to regulate the calcium concentration at appropriate levels necessary for normal cell survival.
iv. The proposed model is the first non-linear spatial model for studying relationships among the parameters like buffers, SERCA pump, ER leak and source influx involved in the calcium homeostasis of an α-cell.
v. Combination of cubic spline and Newton-Raphson method is superior as compared to the other methods like finite element method with linear shape functions, as the proposed approach required less number of elements and less amount of computational effort for solving non-linear reaction-diffusion model as compared to the finite element method with linear shape functions and Gauss elimination method used by most of the earlier research workers for solving linear reaction-diffusion model of calcium homeostasis in various other cells.

The proposed model gives better insight into the role of various parameters in regulating calcium

concentration in an α-cell. This information is crucial in controlling the disorders and diseases caused by the dysfunction of α-cell like diabetes, etc. The model can be applied in the study of diabetes, as it gives information about the factors involved in calcium regulation of α-cell. Calcium directly regulates glucagon secretion through α-cells. So, with the help of the model, it is possible to observe the factors responsible for the disruption of glucagon secretion, which is one of the main factors in regulating the blood glucose level and responsible for the development of diabetes and many other metabolic disorders. The information about the relationships among the various parameters involved in the regulation of calcium level in the α-cell obtained from the proposed model can be useful for developing a framework for the diagnosis and treatment of various disorders like diabetes, etc. The proposed model and approach can also be extended for its applications in various other cells like neurons, astrocytes, myocytes, oocytes, and β-cells for calcium homeostasis and their respective disorders.

5 Appendix

Cubic spline method

The essential idea for using the cubic spline method is to fit a piecewise function with the help of cubic polynomials:

$$Q(x) = \begin{cases} q_1(x), & x \in [x_1, x_2] \\ q_2(x), & x \in [x_1, x_3] \\ & \vdots \\ q_{n-1}(x), & x \in [x_{n-1}, x_n] \end{cases}, \tag{15}$$

$q_j's$ denotes the cubic polynomial and is defined as follows:

$$q_j(x) = a_j(x_j - x)^3 + b_j(x_j - x)^2 + c_j(x_j - x) + d_j, \tag{16}$$

for $j = 1, 2, 3, \cdots, n-1$.
As it is expected that the curve $Q(x)$ must be continuous across its full interval, it follows that each sub-function must connect at the data points,

$$q_j(x_j) = q_{j-1}(x_j), \tag{17}$$

for $j = 2, 3, \cdots, n$.
The derivatives at the data points must also be equal in order for the curve to be smooth over the interval; so,

$$q_j'(x_j) = q_{j-1}'(x_j), \tag{18}$$

for $j = 2, 3, \cdots, n$.
Lastly, since $q_j''(x)$ has to be continuous across the interval,

$$q_j''(j) = q_{j-1}''(x_j),$$

for $j = 1, 2, 3, \cdots, n-1$.
After simplifying the above equations (15), (16), (17) and (18), the cubic spline $Q(x)$ interpolating to the function $y(x)$ at the knots $x_j = x_0 + jh$ for $j = 1, 2, 3, \cdots, n-1$ is given in the interval

$x_{j-1} \leq x \leq x_j$ by the equation,

$$Q(x) = N_{j-1}\frac{(x_j - x)^3}{6h} + N_j\frac{(x - x_{j-1})^3}{6h} + \left(y_{j-1} - \frac{h^2}{6}N_{j-1}\right)\frac{(x_j - x)}{h} + \left(y_j - \frac{h^2}{6}N_j\right)\frac{(x - x_{j-1})}{h}, \tag{19}$$

where $N_j = Q''(x_j)$ and $y_j = y(x_j)$.

$$Q'(x_j^+) = -\frac{h}{3}N_j - \frac{h}{6}N_{j+1} + \frac{y_{j+1} - y_j}{h}, \tag{20}$$

for $j = 0, 1, 2, 3, \cdots, n-1$.

$$Q'(x_j^-) = \frac{h}{3}N_j + \frac{h}{6}N_{j-1} + \frac{y_j - y_{j-1}}{h}, \tag{21}$$

for $j = 1, 2, 3, \cdots, n$. The continuity of the first derivative implies,

$$\frac{h}{6}N_{j-1} + \frac{2h}{3}N_j + \frac{h}{6}N_{j+1} = \frac{y_{j+1} - 2y_j + y_{j-1}}{h}, \tag{22}$$

where $j = 1, 2, 3, \cdots, n-1$ and $h = x_j - x_{j-1}$.

Newton-Raphson method

Consider a non-linear system of equations,

$$\begin{aligned} f_1(x_1, x_2) &= 0, \\ f_2(x_1, x_2) &= 0. \end{aligned} \tag{23}$$

Let $x^{(0)} = (x_1^{(0)}, x_2^{(0)})$ be the initial guess to estimate the solution and f be differentiable at $x^{(0)}$. The equation to the tangent plane to the function $y_i = f_i(x_1, x_2)$ at $x^{(0)}$ for $i = 1, 2$ is,

$$y_i - f_i(x^{(0)}) = \frac{\partial}{\partial x_1}[f_i(x^{(0)})](x_1 - x_1^{(0)}) + \frac{\partial}{\partial x_2}[f_i(x^{(0)})](x_2 - x_2^{(0)}). \tag{24}$$

The above expression can be written in terms of the Jacobian matrix $J(x_1^{(0)}, x_2^{(0)})$ as follows:

$$\begin{bmatrix} y_1 - f_1(x^{(0)}) \\ y_2 - f_2(x^{(0)}) \end{bmatrix} = \begin{bmatrix} \frac{\partial}{\partial x_1}[f_1(x^{(0)})] & \frac{\partial}{\partial x_2}[f_1(x^{(0)})] \\ \frac{\partial}{\partial x_1}[f_2(x^{(0)})] & \frac{\partial}{\partial x_2}[f_2(x^{(0)})] \end{bmatrix} \begin{bmatrix} (x_1 - x_1^{(0)}) \\ (x_2 - x_2^{(0)}) \end{bmatrix}. \tag{25}$$

If the given system is expressed as a vector $V = F(x)$, then from equation (25);

$$\Delta F \approx J(x_1^{(0)}, x_2^{(0)})\Delta X. \tag{26}$$

Suppose that (p_1, p_2) be the solution of equation (23); that is,

$$\begin{aligned} f_1(p_1, p_2) &= 0, \\ f_2(p_1, p_2) &= 0. \end{aligned} \tag{27}$$

To solve the equation (23) using Newton's approach, we must take into account a little change in the function near the coordinates $(p_1^{(0)}, p_2^{(0)})$:

$$\begin{aligned} \Delta y_1 &= y_1 - f_1(x^{(0)}), \qquad & \Delta x_1 &= (x_1 - p_1^{(0)}), \\ \Delta y_2 &= y_2 - f_2(x^{(0)}), \qquad & \Delta x_2 &= (x_2 - p_2^{(0)}). \end{aligned} \tag{28}$$

Set $(x_1^{(0)}, x_2^{(0)}) = (p_1, p_2)$ in equation (23) and use equation (27) to see that $(y_1, y_2) = (0, 0)$. Hence the changes in the dependent variables are:

$$\begin{aligned} y_1 - f_1(x^{(0)}) &= f_1(p_1, p_2) - f_1(p_1^{(0)}, p_2^{(0)}) = 0 - f_1(p_1^{(0)}, p_2^{(0)}), \\ y_2 - f_2(x^{(0)}) &= f_2(p_1, p_2) - f_2(p_1^{(0)}, p_2^{(0)}) = 0 - f_2(p_1^{(0)}, p_2^{(0)}). \end{aligned} \tag{29}$$

Use the result of equation (29) in equation (25) to get the linear transformation,

$$\begin{bmatrix} \frac{\partial}{\partial x_1}[f_1(P_0)] & \frac{\partial}{\partial x_2}[f_1(P_0)] \\ \frac{\partial}{\partial x_1}[f_2(P_0)] & \frac{\partial}{\partial x_2}[f_2(P_0)] \end{bmatrix} \begin{bmatrix} \Delta x_1 \\ \Delta x_2 \end{bmatrix} \approx \begin{bmatrix} f_1(P_0) \\ f_2(P_0) \end{bmatrix}, \tag{30}$$

where $P_0 = (p_1^{(0)}, p_2^{(0)})$. If the Jacobian $J(P_0)$ in (30) is nonsingular, we can solve for

$$\Delta P = [\Delta x_1, \Delta x_2]' = [p_1, p_2]' - [p_1^{(0)}, p_2^{(0)}]'$$

as follows:

$$\Delta P \approx J(P_0)^{-1} F(P_0). \tag{31}$$

Then the next approximation P_1 to the solution P is,

$$P_1 = P_0 + \Delta P = P_0 - J(P_0)^{-1} F(P_0). \tag{32}$$

For a system of n number of equations, Newton's method can be written by generalizing the equation (30).

Declarations

Ethical approval

Not applicable.

Consent for publication

Not applicable.

Conflicts of interest

The authors declare that they have no conflict of interest.

Funding

Not applicable.

Author's contributions

T.S.: Literature Survey, Writing-Original draft preparation. V.: Conceptualization, Methodology, Investigation. N.A.: Visualization, Supervision, Reviewing and Editing. All authors discussed the results and contributed to the final manuscript.

Acknowledgements

Not applicable.

References

[1] Idevall-Hagren, O. and Tengholm, A. Metabolic regulation of calcium signaling in beta cells. *In Seminars in Cell & Developmental Biology*, (Vol. 103, pp. 20-30), Academic Press, (2020). [CrossRef]

[2] Gonzalez-Velez, V., Dupont, G., Gil, A., Gonzalez, A. and Quesada, I. Model for glucagon secretion by pancreatic α -cells. *PLoS One*, 7(3), e32282, (2012). [CrossRef]

[3] Zimny, M.L. and Blackard, W.G. The surface structure of isolated pancreatic islet cells. *Cell and Tissue Research*, 164(4), 467-471, (1975). [CrossRef]

[4] Briant, L., Salehi, A., Vergari, E., Zhang, Q. and Rorsman, P. Glucagon secretion from pancreatic α-cells. *Upsala Journal of Medical Sciences*, 121(2), 113-119, (2016). [CrossRef]

[5] Munoz-Balbontin, M. Criticality control of insulin-release. *In Research Student Conference 2018 Faculty of Technology, Design and Environment Oxford Brookes University Ox*, p. 48, (2018).

[6] Watts, M. and Sherman, A. Modeling the pancreatic α-cell: dual mechanisms of glucose suppression of glucagon secretion. *Biophysical Journal*, 106(3), 741-751, (2014). [CrossRef]

[7] Pathak, K.B. and Adlakha, N. Finite element model to study calcium signalling in cardiac myocytes involving pump, leak and excess buffer. *Journal of Medical Imaging and Health Informatics*, 5(4), 683-688, (2015). [CrossRef]

[8] Pathak, K.B. and Adlakha, N. Finite element model to study one dimensional calcium dyanmics in cardiac myocytes. *Journal of Multiscale Modelling*, 6(02), 1550003, (2015). [CrossRef]

[9] Pathak, K. and Adlakha, N. Finite element model to study two dimensional unsteady state calcium distribution in cardiac myocytes. *Alexandria Journal of Medicine*, 52(3), 261-268, (2016). [CrossRef]

[10] Singh, N. and Adlakha, N. A mathematical model for interdependent calcium and inositol 1, 4, 5-trisphosphate in cardiac myocyte. *Network Modeling Analysis in Health Informatics and Bioinformatics*, 8(1), 18, (2019). [CrossRef]

[11] Singh, N. and Adlakha, N. Nonlinear dynamic modeling of 2-dimensional interdependent calcium and inositol 1, 4, 5-trisphosphate in cardiac myocyte. *Matematicheskaya Biologiya i Bioinformatika*, 14(1), 290-305, (2019). [CrossRef]

[12] Jha, A. and Adlakha, N. Analytical solution of two dimensional unsteady state problem of calcium diffusion in a neuron cell. *Journal of Medical Imaging and Health Informatics*, 4(4), 547-553, (2014). [CrossRef]

[13] Jha, A., Adlakha, N. and Jha, B.K. Finite element model to study effect of $Na^+ - Ca^{2+}$ exchangers and source geometry on calcium dynamics in a neuron cell. *Journal of Mechanics in Medicine and Biology*, 16(02), 1650018, (2016). [CrossRef]

[14] Pawar, A. and Pardasani, K.R. Effect of disturbances in neuronal calcium and IP_3 dynamics on β-amyloid production and degradation. *Cognitive Neurodynamics*, 17(1), 239–256, (2023).

[CrossRef]

[15] Pawar, A. and Raj Pardasani, K. Effects of disorders in interdependent calcium and IP_3 dynamics on nitric oxide production in a neuron cell. *The European Physical Journal Plus*, 137(5), 1-19, (2022). [CrossRef]

[16] Pawar, A. and Pardasani, K.R. Simulation of disturbances in interdependent calcium and β-amyloid dynamics in the nerve cell. *The European Physical Journal Plus*, 137(8), 1-23, (2022). [CrossRef]

[17] Pawar, A. and Pardasani, K.R. Study of disorders in regulatory spatiotemporal neurodynamics of calcium and nitric oxide. *Cognitive Neurodynamics*, (2022). [CrossRef]

[18] Pawar, A. and Pardasani, K.R. Computational model of calcium dynamics-dependent dopamine regulation and dysregulation in a dopaminergic neuron cell. *The European Physical Journal Plus*, 138(1), 30, (2023). [CrossRef]

[19] Tewari, S. and Pardasani, K.R. Finite difference model to study the effects of Na^+ influx on cytosolic Ca^{2+} diffusion. *Biological and Medical Sciences*, 1(04), 205-210, (2008).

[20] Tewari, S. and Pardasani, K.R. Finite element model to study two dimensional unsteady state cytosolic calcium diffusion in presence of excess buffers. *IAENG International Journal of Applied Mathematics*, 40(3), 108-112, (2010).

[21] Tewari, V., Tewari, S. and Pardasani, K.R. A model to study the effect of excess buffers and Na^+ ions on Ca^{2+} diffusion in neuron cell. *International Journal of Bioengineering and Life Sciences*, 5(4), 251-256, (2011).

[22] Tewari, S.G. and Pardasani, K.R. Finite element model to study two dimensional unsteady state cytosolic calcium diffusion. *Journal of Applied Mathematics & Informatics*, 29(1-2), 427-442, (2011).

[23] Tewari, S.G. and Pardasani, K.R. Modeling effect of sodium pump on calcium oscillations in neuron cells. *Journal of Multiscale Modelling*, 4(03), 1250010, (2012). [CrossRef]

[24] Tripathi, A. and Adlakha, N. Finite volume model to study calcium diffusion in neuron cell under excess buffer approximation. *International Journal of Mathematical Sciences and Engineering Applications (IJMSEA)*, 5, 437-447, (2011).

[25] Tripathi, A. and Adlakha, N. Two dimensional coaxial circular elements in FEM to study calcium diffusion in neuron cells. *Applied Mathematical Sciences*, 6(10), 455-466, (2012).

[26] Tripathi, A. and Adlakha, N. Finite element model to study calcium diffusion in a neuron cell involving JRyR, JSerca and JLeak. *Journal of Applied Mathematics & Informatics*, 31(5-6), 695-709, (2013). [CrossRef]

[27] Handy, G., Taheri, M., White, J.A. and Borisyuk, A. Mathematical investigation of IP_3-dependent calcium dynamics in astrocytes. *Journal of Computational Neuroscience*, 42(3), 257-273, (2017). [CrossRef]

[28] Jha, B.K., Adlakha, N. and Mehta, M.N. Finite element model to study calcium diffusion in astrocytes. *International Journal of Pure and Applied Mathematics*, 78(7), 945-955, (2012).

[29] Jha, B.K., Adlakha, N. and Mehta, M.N. Two-dimensional finite element model to study calcium distribution in astrocytes in presence of VGCC and excess buffer. *International Journal of Modeling, Simulation, and Scientific Computing*, 4(02), 1250030, (2013). [CrossRef]

[30] Jha, B.K., Adlakha, N. and Mehta, M.N. Two-dimensional finite element model to study calcium distribution in astrocytes in presence of excess buffer. *International Journal of Biomathe-*

matics, 7(03), 1450031, (2014). [CrossRef]

[31] Jha, B.K., Jha, A. and Adlakha, N. Three-dimensional finite element model to study calcium distribution in astrocytes in presence of VGCC and excess buffer. *Differential Equations and Dynamical Systems*, 28(3), 603-616, (2020). [CrossRef]

[32] Jagtap, Y. and Adlakha, N. Finite volume simulation of two dimensional calcium dynamics in a hepatocyte cell involving buffers and fluxes. *Commun. Math. Biol. Neuroscience*, 2018, (2018). [CrossRef]

[33] Jagtap, Y.D. and Adlakha, N. Simulation of buffered advection diffusion of calcium in a hepatocyte cell. *Matematicheskaya Biologiya i Bioinformatika*, 13(2), 609-619, (2018). [CrossRef]

[34] Jagtap, Y. and Adlakha, N. Numerical study of one-dimensional buffered advection–diffusion of calcium and IP_3 in a hepatocyte cell. *Network Modeling Analysis in Health Informatics and Bioinformatics*, 8(1), 25, (2019). [CrossRef]

[35] Kothiya, A. and Adlakha, N. Model of calcium dynamics regulating IP_3 and ATP production in a fibroblast cell. *Advances in Systems Science and Applications*, 22(3), 49-69, (2022). [CrossRef]

[36] Kotwani, M., Adlakha, N. and Mehta, M.N. Numerical model to study calcium diffusion in fibroblasts cell for one dimensional unsteady state case. *Applied Mathematical Sciences*, 6(102), 5063-5072, (2012).

[37] Kotwani, M., Adlakha, N. and Mehta, M.N. Finite element model to study the effect of buffers, source amplitude and source geometry on spatio-temporal calcium distribution in fibroblast cell. *Journal of Medical Imaging and Health Informatics*, 4(6), 840-847, (2014). [CrossRef]

[38] Kotwani, M. and Adlakha, N. Modeling of endoplasmic reticulum and plasma membrane Ca^{2+} uptake and release fluxes with excess buffer approximation (EBA) in fibroblast cell. *International Journal of Computational Materials Science and Engineering*, 6(01), 1750004, (2017). [CrossRef]

[39] Bhardwaj, H. and Adlakha, N. Radial basis function based differential quadrature approach to study reaction diffusion of Ca^{2+} in T lymphocyte. *International Journal of Computational Methods*, (2022). [CrossRef]

[40] Naik, P.A. and Zu, J. Modeling and simulation of spatial-temporal calcium distribution in T lymphocyte cell by using a reaction-diffusion equation. *Journal of Bioinformatics and Computational Biology*, 18(02), 2050013, (2020). [CrossRef]

[41] Naik, P.A. and Pardasani, K.R. Finite element model to study effect of Na^+/K^+ pump and Na^+/Ca^{2+} exchanger on calcium distribution in oocytes in presence of buffers. *Asian Journal of Mathematics & Statistics*, 7(1), 21, (2014).

[42] Naik, P.A. and Pardasani, K.R. One dimensional finite element model to study calcium distribution in oocytes in presence of VGCC, RyR and buffers. *Journal of Medical Imaging and Health Informatics*, 5(3), 471-476, (2015). [CrossRef]

[43] Naik, P.A. and Pardasani, K.R. Two dimensional finite element model to study calcium distribution in oocytes. *Journal of Multiscale Modelling*, 6(01), 1450002, (2015). [CrossRef]

[44] Naik, P.A. and Pardasani, K.R. Finite element model to study calcium distribution in oocytes involving voltage gated Ca^{2+} channel, ryanodine receptor and buffers. *Alexandria Journal of Medicine*, 52(1), 43-49, (2016). [CrossRef]

[45] Naik, P.A. and Pardasani, K.R. 2D finite-element analysis of calcium distribution in oocytes. *Network Modeling Analysis in Health Informatics and Bioinformatics*, 7(1), 1-11, (2018). [CrossRef]

[46] Naik, P.A. and Pardasani, K.R. Three-dimensional finite element model to study effect of RyR calcium channel, ER leak and SERCA pump on calcium distribution in oocyte cell. *International Journal of Computational Methods*, 16(01), 1850091, (2019). [CrossRef]

[47] Panday, S. and Pardasani, K.R. Finite element model to study effect of advection diffusion and Na^+/Ca^{2+} exchanger on Ca^{2+} distribution in oocytes. *Journal of Medical Imaging and Health Informatics*, 3(3), 374-379, (2013). [CrossRef]

[48] Panday, S. and Pardasani, K.R. Finite element model to study the mechanics of calcium regulation in oocyte. *Journal of Mechanics in Medicine and Biology*, 14(02), 1450022, (2014). [CrossRef]

[49] Manhas, N. and Pardasani, K.R. Mathematical model to study IP_3 dynamics dependent calcium oscillations in pancreatic acinar cells. *Journal of Medical Imaging and Health Informatics*, 4(6), 874-880, (2014). [CrossRef]

[50] Manhas, N. and Pardasani, K.R. Modelling mechanism of calcium oscillations in pancreatic acinar cells. *Journal of Bioenergetics and Biomembranes*, 46, 403-420, (2014). [CrossRef]

[51] Manhas, N., Sneyd, J. and Pardasani, K.R. Modelling the transition from simple to complex Ca^{2+} oscillations in pancreatic acinar cells. *Journal of Biosciences*, 39(3), 463-484, (2014). [CrossRef]

[52] Jha, A., & Adlakha, N. Finite element model to study the effect of exogenous buffer on calcium dynamics in dendritic spines. *International Journal of Modeling, Simulation, and Scientific Computing*, 5(02), 1350027, (2014). [CrossRef]

[53] Wiesner, T.F., Berk, B.C. and Nerem, R.M. A mathematical model of cytosolic calcium dynamics in human umbilical vein endothelial cells. *American Journal of Physiology-Cell Physiology*, 270(5), C1556-C1569, (1996). [CrossRef]

[54] Futagi, D. and Kitano, K. Ryanodine-receptor-driven intracellular calcium dynamics underlying spatial association of synaptic plasticity. *Journal of Computational Neuroscience*, 39(3), 329-347, (2015). [CrossRef]

[55] Joshi, H. and Jha, B.K. Fractional reaction diffusion model for Parkinson's disease. *In Proceedings of the International Conference on ISMAC in Computational Vision and Bio-Engineering 2018 (ISMAC-CVB)*, pp. 1739-1748, Springer International Publishing, (2019). [CrossRef]

[56] Joshi, H. and Jha, B.K. Chaos of calcium diffusion in Parkinson's infectious disease model and treatment mechanism via Hilfer fractional derivative. *Mathematical Modelling and Numerical Simulation with Applications*, 1(2), 84-94, (2021). [CrossRef]

[57] Joshi, H. and Jha, B.K. 2D dynamic analysis of the disturbances in the calcium neuronal model and its implications in neurodegenerative disease. *Cognitive Neurodynamics*, (2022). [CrossRef]

[58] Joshi, H. and Jha, B.K. 2D memory-based mathematical analysis for the combined impact of calcium influx and efflux on nerve cells. *Computers & Mathematics with Applications*, 134, 33-44, (2023). [CrossRef]

[59] Kahn, S.E., Zraika, S., Utzschneider, K.M. and Hull, R.L. The beta cell lesion in type 2 diabetes: there has to be a primary functional abnormality. *Diabetologia*, 52(6), 1003-1012, (2009). [CrossRef]

[60] Bertram, R., Sherman, A. and Satin, L.S. Metabolic and electrical oscillations: partners in controlling pulsatile insulin secretion. *American Journal of Physiology-Endocrinology And Metabolism*, 293(4), E890-E900, (2007). [CrossRef]

[61] Pedersen, M.G., Cortese, G. and Eliasson, L. Mathematical modeling and statistical analysis

of calcium-regulated insulin granule exocytosis in β-cells from mice and humans. *Progress in Biophysics and Molecular Biology*, 107(2), 257-264, (2011). [CrossRef]

[62] Diderichsen, P.M. and Göpel, S.O. Modelling the electrical activity of pancreatic α-cells based on experimental data from intact mouse islets. *Journal of Biological Physics*, 32, 209-229, (2006). [CrossRef]

[63] Fridlyand, L.E. and Philipson, L.H. A computational systems analysis of factors regulating α-cell glucagon secretion. *Islets*, 4(4), 262-283, (2012). [CrossRef]

[64] Montefusco, F. and Pedersen, M.G. Mathematical modelling of local calcium and regulated exocytosis during inhibition and stimulation of glucagon secretion from pancreatic alpha cells. *The Journal of Physiology*, 593(20), 4519-4530, (2015). [CrossRef]

[65] Brereton, M.F., Vergari, E., Zhang, Q. and Clark, A. Alpha-, delta-and PP-cells: are they the architectural cornerstones of islet structure and co-ordination?. *Journal of Histochemistry & Cytochemistry*, 63(8), 575-591, (2015). [CrossRef]

[66] Moede, T., Leibiger, I.B. and Berggren, P.O. Alpha cell regulation of beta cell function. *Diabetologia*, 63(10), 2064-2075, (2020). [CrossRef]

[67] Crank, J. *The Mathematics of Diffusion, Second Edition* (Vol. 4). Clarendon Press Oxford, (1975).

[68] Smith, G.D. Modeling local and global calcium signals using reaction diffusion equations. *Computational neuroscience*, 49-85, (2001).

[69] Dupont, G., Falcke, M., Kirk, V. and Sneyd, J. *Models of Calcium Signalling* (Vol. 43). Springer: New York, USA, (2016). [CrossRef]

[70] Albasiny, E.L. and Hoskins, W.D. Cubic spline solutions to two-point boundary value problems. *The Computer Journal*, 12(2), 151-153, (1969). [CrossRef]

[71] McKinley, S., Levine, M. Cubic spline interpolation. *College of the Redwoods*, 45(1), 1049-1060, (1998).

Bulletin of Biomathematics (BBM)
(https://bulletinbiomath.org)

How to cite this article: Singh, T., Vaishali & Adlakha, N. (2023). Numerical investigations and simulation of calcium distribution in the alpha-cell. *Bulletin of Biomathematics*, 1(1), 40-57. https://doi.org/10.59292/bulletinbiomath.2023003